Particle Accelerators, 1985, Vol. 17, pp. 227–242
0031-2460/85/1704–0227/$20.00/0

Printed in the United States of America

ON THE UNIQUE NUMERICAL SOLUTION OF MAXWELLIAN EIGENVALUE PROBLEMS IN THREE DIMENSIONS

T. WEILAND

Deutsches Elektronen-Synchrotron DESY, Hamburg

The numerical computation of eigensolutions of Maxwell's equations in some volume of space does not necessarily yield unique solutions, especially when applied to three-dimensional problems. Thus an accurate calculation can become extremely difficult and the results uncertain.

This problem can be overcome by using a special finite-difference method that solves all the four Maxwell equations in a consistent way, so that the properties of the differential equations and their solutions are still exhibited in the grid space for the corresponding matrix equations and their discrete solutions. By utilizing a simple combination of Maxwell's equations in the grid space, we find a matrix representation with non-vanishing eigenvalues and thus unique solutions. This matrix equation corresponds to the wave equation in free space.

Numerical examples prove the stability and simplicity of the algorithm as well as the accuracy in comparison with measurements.

LIST OF SYMBOLS

Z_0, Y_0	free space impedance, admittance $Z_0 Y_0 = 1$, $Z_0 = \sqrt{\mu_0/\varepsilon_0}$
μ_0, ε_0	permeability, permittivity of vacuum
μ_r, ε_r	relative permeability, permittivity
μ, ε	permeability, permittivity, $\mu = \mu_r\mu_0$, $\varepsilon = \varepsilon_r\varepsilon_0$
ω	circular frequency
c	speed of light in vacuum
$\underline{\mathbf{E}}$, $\underline{\mathbf{H}}$	vector of electric/magnetic field
$\underline{\mathbf{D}}$, $\underline{\mathbf{B}}$	vector of electric/magnetic flux density
$\mathbf{E}$, $\mathbf{H}$, $\mathbf{D}$, $\mathbf{B}$, $\mathbf{J}$	normalized vectors, e.g. $\underline{\mathbf{E}} = \mathbf{E}\sqrt{Z_0}\sin\omega t$, $\underline{\mathbf{H}} = \mathbf{H}\sqrt{Y_0}\cos\omega t$
$\mathbf{e}$, $\mathbf{h}$	vector holding all electric/magnetic field components in the grid
$\mathbf{d}$, $\mathbf{b}$	vector holding all electric/magnetic flux densities
$\mathbf{G}$, $\tilde{\mathbf{G}}$	grid, dual grid
M_u, M_v, M_w	index increments for linear numbering
u, v, w	orthogonal coordinates
$\mathbf{D}_A$, $\mathbf{D}_{\tilde{A}}$	diagonal matrix holding cell areas in $\mathbf{G}$, $\tilde{\mathbf{G}}$
$\mathbf{D}_s$, $\mathbf{D}_{\tilde{s}}$	diagonal matrix holding step sizes in $\mathbf{G}$, $\tilde{\mathbf{G}}$
$\mathbf{D}_V$	diagonal matrix with volume of grid cells
$\mathbf{D}_\varepsilon$, $\mathbf{D}_\mu$	diagonal matrix with permittivities/permeabilities
$\mathbf{A}_u$, $\mathbf{A}_v$, $\mathbf{A}_w$	basic discretization matrix, $N \times N$

$\mathbf{C}$	discrete curl operator in grid space $\mathbf{G}$
$\mathbf{C}^*$	transpose of $\mathbf{C}$ = discrete curl operator in dual grid $\tilde{\mathbf{G}}$
$\mathbf{S}$	discrete div operator in grid space $\mathbf{G}$
$\mathbf{D}_\delta$	Kronecker diagonal matrix with 1 on free space grid nodes, else 0
s	penalty parameter

INTRODUCTION

We consider solutions of Maxwell's equations with harmonic time dependence. Thus we may write Maxwell's equations for loss-free materials without any further restriction as

$$\operatorname{curl} \mathbf{H} = \frac{\omega}{c} \varepsilon_r \mathbf{E}, \tag{1}$$

$$\operatorname{curl} \mathbf{E} = \frac{\omega}{c} \mu_r \mathbf{H}, \tag{2}$$

$$\operatorname{div} \varepsilon_r \mathbf{E} = 0, \tag{3}$$

$$\operatorname{div} \mu_r \mathbf{H} = 0. \tag{4}$$

For given geometry, distribution of ε_r and μ_r, and boundary conditions, we are interested in eigensolutions of the above system for the lowest few eigenvalues. Practical examples for this problem can be found wherever rf resonators are used that do not have higher symmetries. In this paper we focus on fully three-dimensional problems — the two- and quasi two-dimensional cases can be considered to be solved.[1]

Various numerical methods have been proposed in the last decade for discretizing the problem.[2–4] However, none of the algorithms has been free of severe numerical problems caused by a mixing of eigensolutions with irrotational solutions. This was especially true when three-dimensional problems were attacked and the appearance of "ghost modes" left the judgement of whether a solution was correct or not to the user. This in fact is an unsatisfactory procedure.

The appearance of non-unique solutions is basically due to the fact that solving Maxwell's curl equations (1) and (2) combined as

$$\operatorname{curl} \frac{1}{\mu_r} \operatorname{curl} \mathbf{E} = \left(\frac{\omega}{c}\right)^2 \varepsilon_r \mathbf{E} \tag{5}$$

yields two distinct groups of solutions:

a) $\omega \equiv 0$, $\operatorname{curl} \mathbf{E} = 0$, static fields

b) $\omega \neq 0$, resonant solutions.

The fact that there exist trivial ($\omega = 0$) solutions of Eq. (5) implies that the discretized equation will have a matrix with vanishing eigenvalues. Thus discretized solutions for $\omega \neq 0$ are not unique and are in general a mixture with all possible static fields. In addition, any numerical treatment of Eq. (5) is rather

difficult. When the metallic boundaries are simply connected, such irrotational fields can be caused only by real electric charges on non-conducting surfaces.

Analytically, the problem may be solved by imposing an additional constraint on the fields

$$\operatorname{div} \varepsilon_r \mathbf{E} = 0. \tag{6}$$

This condition excludes all irrotational solutions, in particular those with static content — for simply connected regions. The way of combining Eqs. (6) and (5) is somewhat arbitrary. Using the "penalty parameter" s one can write[4]

$$\operatorname{curl} \frac{1}{\mu_r} \operatorname{curl} \mathbf{E} - s \operatorname{grad} \operatorname{div} \varepsilon_r \mathbf{E} = \left(\frac{\omega}{c}\right)^2 \varepsilon_r \mathbf{E}. \tag{7}$$

By solving the above equations for various numerical values of s, one finds solutions that do not depend on s and thus can be considered "good solutions". Since one has to undertake many computations and each one is extremely time-consuming, the situation remains unsatisfactory.

For $s = 1$, $\varepsilon_r = 1$ and $\mu_r = 1$, we obtain the wave equation

$$\nabla^2 \mathbf{E} + \left(\frac{\omega}{c}\right)^2 \mathbf{E} = \mathbf{0}, \tag{8}$$

with $\operatorname{div} \varepsilon_r \mathbf{E} = 0$ on the boundary. This equation offers a simple way of avoiding irrotational solutions. Though restricted to the case of the vacuum with metallic boundaries but without material insertions, this way promises unique numerical solutions for many realistic problems.

However, it has been found that the discretization of the wave equation can still yield "unphysical" solutions or "ghost modes".[3] The reason for this is that not every numerical discretization method is consistent with Maxwell's equations in the sense that the analytical properties are transferred to the grid solutions. Thus, severe difficulties arise when standard discretization methods are applied to Maxwell's vector-field problems, especially when complicated boundary conditions are present.

In this paper, we describe a consistent algorithm (FIT-method[5,6]) that has been applied previously to many field problems. This algorithm produces a matrix equation for each of the four Maxwell's equations. The combination of the matrix equations yields a symmetric operator having unique solutions in the grid space.

The key point of the method is that all four Maxwell's equations are discretized in a consistent way, i.e., time-harmonic fields that are source-free in the real space also are source-free in the grid space. Thus it is easy to eliminate all irrotational field contents that cause non-unique solutions in other algorithms.

It is shown (Appendix A) that every grid solution of Eq. (5) is source-free in the grid space. The transformation of Eq. (5) to Eq. (7) is done in the grid space except at the boundary. Thus, we have $\operatorname{div} \varepsilon_r \mathbf{E} = 0$ at the boundary and find a complete base without irrotational modes. The method works in any orthonormal coordinate system and includes arbitrary distributions of permittive and permeable material in the region of solution.

THE METHOD

We use a topologically regular grid **G** in an orthonormal coordinate system (u, v, w) defined as

$$\begin{aligned}\mathbf{G} = \{(u_i, v_j, w_k) \in \mathbf{R}^3;\ & u_1 \le u_i \le u_I,\ i = 1, \ldots, I \\ & v_1 \le v_j \le v_J,\ j = 1, \ldots, J \\ & w_1 \le w_k \le w_K,\ k = 1, \ldots, K\}.\end{aligned} \tag{9}$$

We use a linear numbering system for the grid nodes

$$n = 1 + (i-1) \cdot M_u + (j-1) \cdot M_v + (k-1) \cdot M_w \tag{10}$$

with $n = 1, \ldots, N$; $N = I \cdot J \cdot K$ and

$$M_u = 1, \qquad M_v = I, \qquad M_w = I \cdot J, \tag{11}$$

or any permutation of the latter three assignments. Figure 1 shows a sketch of such a topological grid.

We then have to allocate components of the unknown fields or vector potentials to the grid and we use the FIT algorithm[5,6] that allocates different components of the electric field to different locations in **G** as shown in Figure 2. This method also uses a dual grid $\tilde{\mathbf{G}}$ in which the components of the magnetic field are assigned in the same way as the electric field is in **G** (for more details see Refs. 5 and 6).

An approximate solution of Maxwell's equation may be obtained by evaluating the integrals along the circumference of each grid cell surface in first order

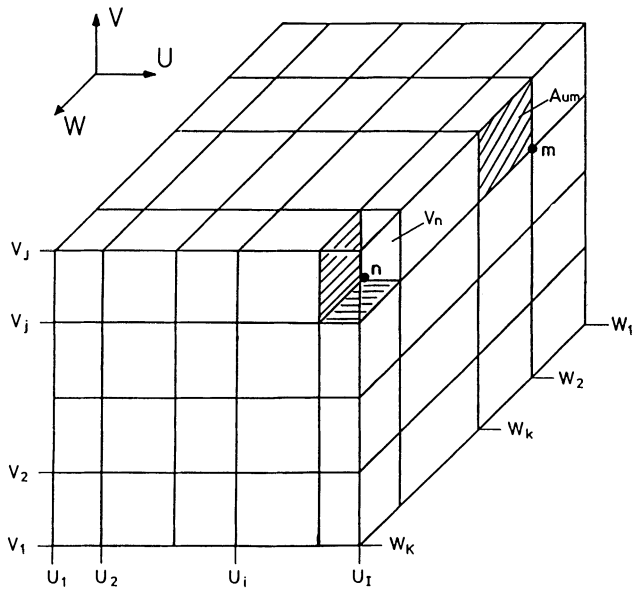

FIGURE 1 Topologically regular grid in three dimensions.

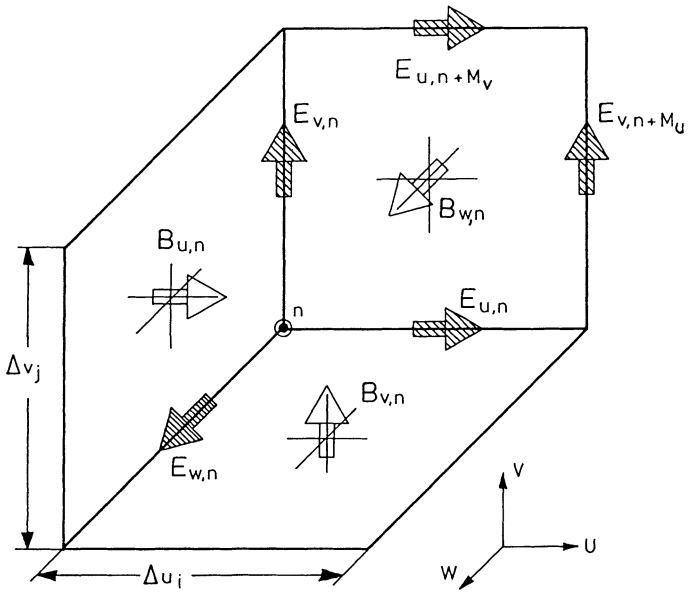

FIGURE 2 The allocation of unknown field components in the grid.

approximation. Solving Eq. (2) in integral form,

$$\oint \mathbf{E} \cdot d\mathbf{s} = \frac{\omega}{c} \int\int \mathbf{B} \cdot d\mathbf{A} \tag{12}$$

over the cell surface perpendicular to the w-axis shown in Fig. 2 yields

$$(u_{i+1} - u_i) \cdot (E_{u,n} - E_{u,n+M_v}) + (v_{j+1} - v_j) \cdot (E_{v,n+M_u} - E_{v,n}) = \frac{\omega}{c} (u_{i+1} - u_i) \cdot (v_{j+1} - v_j) \cdot B_{w,n}. \tag{13}$$

In order to get more insight into the algebraic structure of this algorithm, we must introduce a few definitions.

Putting all unknown components of the fields into column vectors yields

$$\mathbf{e} = (E_{u_1}, E_{u_2}, \ldots, E_{uN}, E_{v_1} \ldots E_{wN})^* \tag{14}$$

$$\mathbf{b} = (B_{u_1}, B_{u_2}, \ldots, B_{uN}, B_{v_1} \ldots B_{wN})^* \tag{15}$$

The mesh step sizes occurring in Eq. (13) are put into a $3N \times 3N$ diagonal matrix

$$D_s = \text{Diag}\{(u_2 - u_1), \ldots, (u_I - u_{I-1}), 0, (u_2 - u_1), \ldots, (w_K - w_{K-1}), 0\}, \tag{16}$$

each element of which contains the step-size value for the electric-field component along that grid element.

Similarly we can define a diagonal matrix $\mathbf{D}_A$ containing all the cell surface areas that belong to the components of the magnetic field (see Fig. 1). Finally, we define the band matrix (of dimensions $N \times N$)

$$\mathbf{A}_u = \begin{pmatrix} & & & & 0 \\ & 0 & 1 & & \\ 0 & & -1 & & \\ & \longrightarrow & & \longleftarrow & \\ & & M_u & & \end{pmatrix}, \tag{17}$$

which enables us to write the matrix equation representing Eq. (13) at all grid nodes in a simple algebraic matrix occurring in Eq. (18). The matrix $\mathbf{A}_u$ has only two bands at a distance M_u given by the definition of the linear numbering system, Eqs. (10) and (11).

We now can write down the analogue of Maxwell's Eq. (2) in the grid space as

$$\begin{pmatrix} \mathbf{0} & \mathbf{A}_w^* & -\mathbf{A}_v^* \\ -\mathbf{A}_w^* & \mathbf{0} & \mathbf{A}_u^* \\ \mathbf{A}_v^* & -\mathbf{A}_u^* & \mathbf{0} \end{pmatrix} \cdot \mathbf{D}_s \mathbf{e} = \left(\frac{\omega}{c}\right) \mathbf{D}_A \mathbf{b} \tag{18}$$

In order to introduce the distribution of material in the grid space, we define diagonal matrices correlating the field strengths and the flux densities in the grid space

$$\mathbf{b} = \mathbf{D}_\mu \mathbf{h} \leftrightarrow \mathbf{B} = \mu \cdot \mathbf{H} \tag{19}$$

$$\mathbf{d} = \mathbf{D}_\varepsilon \mathbf{e} \leftrightarrow \mathbf{D} = \varepsilon \cdot \mathbf{E}. \tag{20}$$

Performing the same procedure for the first Maxwell equation and replacing the grid quantities in $\mathbf{G}$ by those in the dual grid $\tilde{\mathbf{G}}$ (see for more details Refs. 5 and 6), we obtain

$$\begin{pmatrix} \mathbf{0} & -\mathbf{A}_w & \mathbf{A}_v \\ \mathbf{A}_w & \mathbf{0} & -\mathbf{A}_u \\ -\mathbf{A}_v & \mathbf{A}_u & \mathbf{0} \end{pmatrix} \cdot \mathbf{D}_{\tilde{s}} \mathbf{D}_\mu^{-1} \mathbf{b} = \left(\frac{\omega}{c}\right) \mathbf{D}_{\tilde{A}} \mathbf{D}_\varepsilon \mathbf{e}. \tag{21}$$

These equations also contain the rows and columns that belong to already known components e.g. those vanishing due to boundary conditions. This is done in order to maintain the simple algebraic structure of the matrices. However, in a computer code, one can always compress the equations in such a way that they only have real unknowns to work on.

Using the abbreviation C for the algebraic curl operator

$$\mathbf{C} = \begin{pmatrix} \mathbf{0} & -\mathbf{A}_w & \mathbf{A}_v \\ \mathbf{A}_w & \mathbf{0} & -\mathbf{A}_u \\ -\mathbf{A}_v & \mathbf{A}_u & \mathbf{0} \end{pmatrix}, \tag{22}$$

we can combine Eqs. (18) and (21) to give

$$\left(\frac{\omega}{c}\right)^2 \cdot \mathbf{D}_\varepsilon \cdot \mathbf{D}_{\tilde{A}} \cdot \mathbf{e} = \mathbf{C}\mathbf{D}_\mu^{-1}\mathbf{D}_{\tilde{s}}\mathbf{D}_A^{-1}\mathbf{C}^*\mathbf{D}_s\mathbf{e} \tag{23}$$

This is an algebraic eigenvalue equation for the unknown electric-field components with an asymmetric matrix. However, we find that the system matrix is topologically symmetric. In the case of a uniform medium and a regularly spaced grid we find

$$\begin{aligned} &\mathbf{D}_\varepsilon = \mathbf{D}_\mu = \mathbf{D}_A = \mathbf{D}_{\tilde{A}} = \mathbf{D}_s = \mathbf{D}_{\tilde{s}} = \text{unit matrix} \\ &\left(\frac{\omega}{c}\right)^2 \cdot \mathbf{e} = \mathbf{C}\mathbf{C}^*\mathbf{e} \end{aligned} \tag{24}$$

In order to convert the algorithm into a symmetric form in the general case we must perform a diagonal transformation, which physically replaces the field strength by the local density of the stored energy

$$\mathbf{e}' = (\mathbf{D}_\varepsilon \mathbf{D}_{\tilde{A}} \mathbf{D}_s)^{1/2}\mathbf{e}. \tag{25}$$

Now, instead of Eq. (3) we obtain

$$\left(\frac{\omega}{c}\right)^2 \mathbf{e}' = (\tilde{\mathbf{D}}\mathbf{C}\mathbf{D})(\tilde{\mathbf{D}}\mathbf{C}\mathbf{D})^*\mathbf{e}', \tag{26}$$

using the abbreviation

$$\mathbf{D} = \mathbf{D}_\mu^{-1/2}\mathbf{D}_{\tilde{s}}^{1/2}\mathbf{D}_A^{-1/2} \tag{27}$$

$$\tilde{\mathbf{D}} = \mathbf{D}_\varepsilon^{-1/2}\mathbf{D}_s^{1/2}\mathbf{D}_{\tilde{A}}^{-1/2}. \tag{28}$$

Equation (26) is finally symmetric and has some remarkable properties:

- $\mathbf{C}$ is a canonical matrix with elements taking only the values $+1$, -1 or 0.
- All information about mesh step sizes and material distribution is contained in diagonal matrices ($\mathbf{D}$, $\tilde{\mathbf{D}}$).
- The matrix is symmetric and thus we have only real values for ω^2.

However, as mentioned earlier, the eigenvalue equation not only has $\omega \neq 0$ solutions, but also describes static solutions with $\omega \equiv 0$ (see Appendix A). When the metallic boundaries are simply connected, such fields can be caused only by real electric charges on non-conducting surfaces. Thus we can avoid these solutions by imposing the condition (6) on Eq. (26). To do this, we discretize the equation

$$\text{div } \varepsilon_r \mathbf{E} = \rho, \tag{29}$$

Defining $\mathbf{q}$ as a vector of dimension N containing the values of the charges on each grid node we find that the discretized form of Eq. (29) reads simply

$$(\mathbf{A}_u \,\vdots\, \mathbf{A}_v \,\vdots\, \mathbf{A}_w) \cdot \mathbf{D}_\varepsilon \mathbf{D}_{\tilde{A}} \mathbf{e} = \mathbf{q}, \tag{30}$$

This equation can be easily understood using Fig. 3. In order to construct a $3N$ by $3N$ matrix equation from Eq. (30) and to combine it with Eq. (26), we define

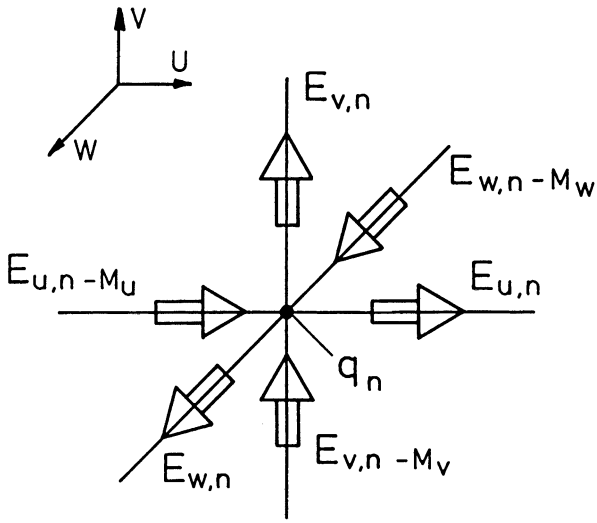

FIGURE 3 Six electric field components contributing to the charge q_n on node number n.

another diagonal matrix

$$\mathbf{D}_V = \text{Diag}\{V_1, \ldots, V_N, V_1, \ldots, V_N, V_1, \ldots V_N\} \tag{31}$$

that holds all volume elements three times, one for each component.

The matrix $\mathbf{S} = (\mathbf{A}_u \mid \mathbf{A}_v \mid \mathbf{A}_w)$ of order $N \times 3N$ in Eq. (30) is used to construct a symmetric $3N$ by $3N$ equation for the transformed field components

$$\tilde{\mathbf{D}}^{-1}\mathbf{S}^*\mathbf{D}_V^{-1}\mathbf{S}\tilde{\mathbf{D}}^{-1}\mathbf{e}' = \mathbf{q}'. \tag{32}$$

We now define a Kronecker matrix $\mathbf{D}_N$ with 1 for mesh points that do not lie on a metallic boundary and with a zero for all nodes on a metallic boundary and the $3N \times 3N$ matrix $\mathbf{D}_\delta = (\mathbf{D}_N, \mathbf{D}_N, \mathbf{D}_N)$. Then we can transform Eq. (32) into

$$\mathbf{D}_\delta\tilde{\mathbf{D}}^{-1}\mathbf{S}^*\mathbf{D}_V^{-1}\mathbf{S}\tilde{\mathbf{D}}^{-1}\mathbf{D}_\delta\mathbf{e}' = \mathbf{0}. \tag{33}$$

This equation explicitly imposes the condition on the electric field that there are no charges in free space and thus excludes irrotational solutions. Note that this equation is equivalent to the replacement

$$\text{grad div } \varepsilon_r\mathbf{E} \leftrightarrow \mathbf{D}_\delta\tilde{\mathbf{D}}^{-1}\mathbf{S}^*\mathbf{D}_V^{-1}\mathbf{S}\tilde{\mathbf{D}}^{-1}\mathbf{D}_\delta \cdot \mathbf{e}' \tag{34}$$

Finally, we combine the discrete curl-curl operator and the source equation to give

$$[(\tilde{\mathbf{D}}\mathbf{C}\mathbf{D}) \cdot (\tilde{\mathbf{D}}\mathbf{C}\mathbf{D})^* + (\mathbf{D}_V^{-1/2}\mathbf{S}\tilde{\mathbf{D}}^{-1}\mathbf{D}_\delta)^* \cdot (\mathbf{D}_V^{-1/2}\mathbf{S}\tilde{\mathbf{D}}^{-1}\mathbf{D}_\delta)]\mathbf{e}' = \left(\frac{\omega}{c}\right)^2\mathbf{e}'. \tag{35}$$

The Kronecker matrix guarantees that the equations remain unchanged at the boundary. Thus, we implicitly have source-free fields at the boundary (Appendix

A). Solutions of Eq. (35) fulfill the condition $\omega^2 \in \mathbf{R}$, and form a complete basis. In fact, it can be shown (Appendix B) that $\omega^2 \geqq 0$ and thus that all frequencies ω are real.

The discrete operator has the following remarkable properties:

1. The global structure is given by

$$\mathbf{B}\mathbf{e}' = \left(\frac{\omega}{c}\right)^2 \mathbf{e}', \qquad \mathbf{B} = \begin{pmatrix} \mathbf{B}_{uu} & \mathbf{B}_{uv} & \mathbf{B}_{uw} \\ \mathbf{B}_{uv}^* & \mathbf{B}_{vv} & \mathbf{B}_{vw} \\ \mathbf{B}_{uw}^* & \mathbf{B}_{vw}^* & \mathbf{B}_{ww} \end{pmatrix}$$

2. The matrix is real and symmetric.
3. The matrix is semi-definite.
   (Though not strictly proven, it is obvious from the above that the matrix is in fact positive-definite for simply connected regions.)
4. The matrix is composed of simple products and sums of canonical operators. Mesh step sizes and material properties are kept in separate diagonal matrices.
5. All logical connections are based on one single difference operator matrix with two bands: see Eq. (17).

One other very interesting property of the final matrix is that for the simplified cases of free space and homogeneous media, all elements in the coupling matrices $\mathbf{B}_{uv}$, $\mathbf{B}_{uw}$ and $\mathbf{B}_{vw}$ vanish. Thus we have three independent equations that are coupled only at the boundary or at any location where the material property changes. In the case of free space, the diagonal main matrices $\mathbf{B}_{uu}$, $\mathbf{B}_{vv}$ and $\mathbf{B}_{ww}$ turn into the well-known discrete ∇^2 operator with a 6 on the diagonal and six times -1 on side diagonals.

This way of deriving the final matrix step by step appears to be rather complicated. However, a direct discretization for the general case of Eq. (5) seems to be much more complicated. The way described here needs only very basic operations since the final matrix is composed of a number of rather simple matrices. Last but not least, this method guarantees that there exist only physical and non-trivial solutions since Eq. (6) is imposed implicitly at the boundary.

APPLICATION

A preliminary version of a three-dimensional computer program has been prepared. The code allows for arbitrarily shaped structures with material insertions of permittive and/or permeable material. The examples presented here serve only as a proof of principle.

We first consider a cylindrically symmetric cavity with beam tubes as shown in Fig. 4. Figure 5 shows the representation of this cavity on a $40 \times 40 \times 40$ grid. For the actual calculation, however, we use only one-eighth and make use of the symmetry as shown in Fig. 6. Thus one has to run the code several times for the

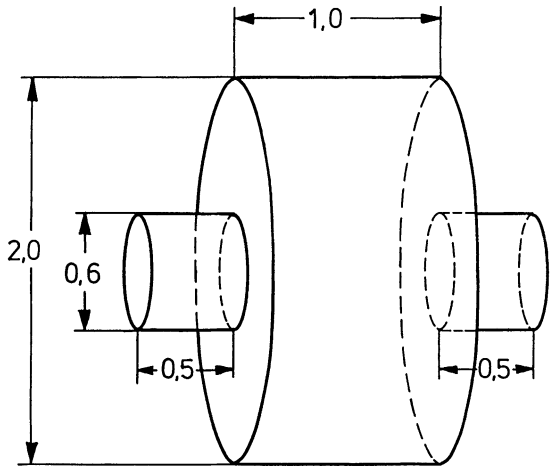

FIGURE 4 Cylindrical cavity with beam tubes.

same geometry but with different boundary conditions on the planes of symmetry. This example has been chosen since it is possible to calculate the eigenfrequencies quite accurately with the $2D$-code URMEL[7] (which makes use of the cylindrical symmetry and uses only a $2D$ grid). Table I shows the lowest modes found with both codes.

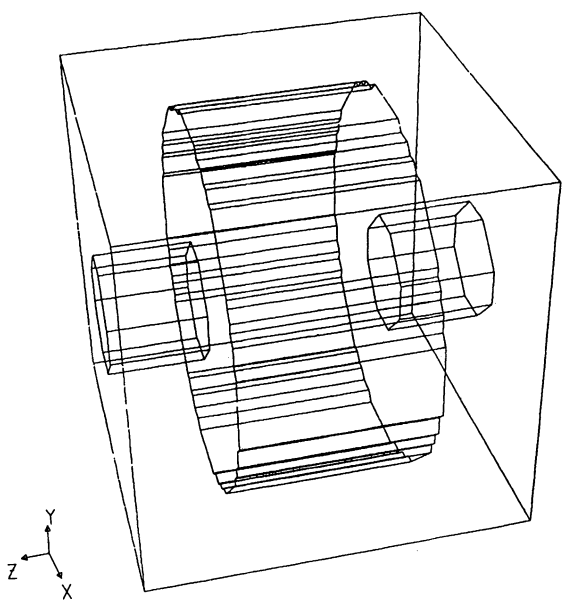

FIGURE 5 Mesh representation of the cylindrical cavity in a $40\times40\times40$ grid.

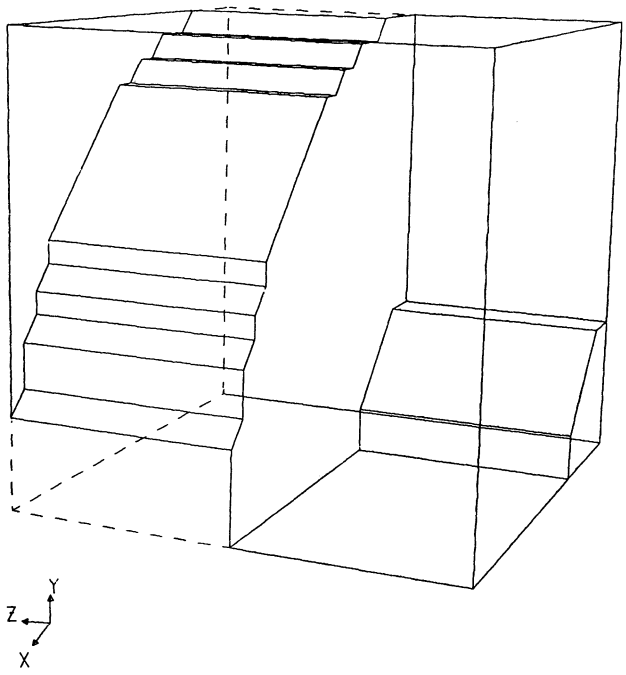

FIGURE 6 One eighth of the cylindrical cavity used for the calculation.

The URMEL[7] results are obtained for a plane grid of 5000 nodes giving a relative accuracy of 10^{-4}. Azimuthal mode numbers up to quadrupole ($m = 0, 1, 2$) were used.

For comparison with some measured results, we use the cavity shown in Fig. 7, a rectangular cavity with a rectangular post in the center. The two lowest modes have been measured[8] and Table II shows a comparison with calculated data.

TABLE I

Lowest Modes in a Cylindrical Cavity with Side Tubes Found Using the 2*D*-Code URMEL and by the Three-Dimensional Calculation

	f/MHz		
Mode Type*	URMEL $N_2 = 5000$	3*D*-calculation $N_3 = 21^3 = 9261$	Relative Error
TMØ-EE-1	116.53	116.76	$1.7 \cdot 10^{-3}$
1-ME-1	168.23	168.30	$4.2 \cdot 10^{-4}$
1-EE-1	179.14	179.24	$5.6 \cdot 10^{-4}$
TMØ-ME-1	190.76	190.71	$2.6 \cdot 10^{-4}$
2-ME-1	208.67	208.87	$9.6 \cdot 10^{-4}$
1-ME-2	225.97	226.30	$1.5 \cdot 10^{-3}$
2-EE-1	244.02	243.97	$2.0 \cdot 10^{-4}$

* For notation, see Ref. 7.

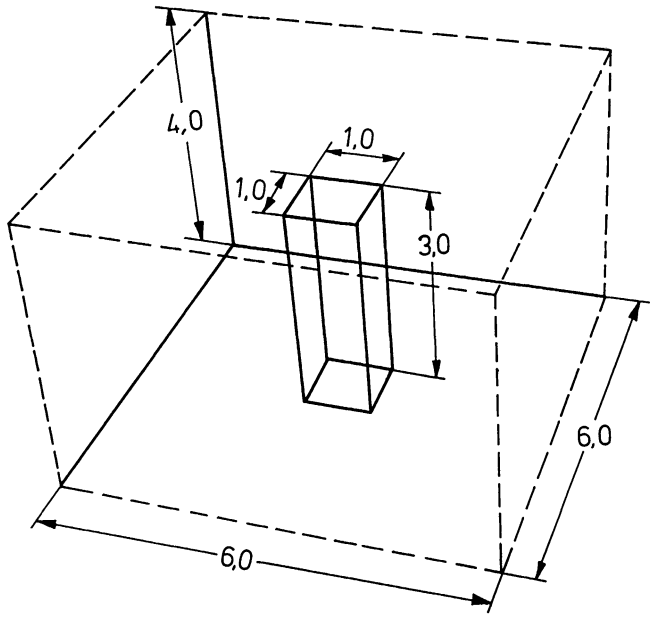

FIGURE 7 Simple rectangular cavity with metallic post.

TABLE II

Lowest Modes in a Three-Dimensional Rectangular Cavity as Measured and Calculated (Only One-quarter was Used in the Calculation with $N_3 = 12 \cdot 16 \cdot 12 = 2304$).

Mode #	Calculated Frequency (MHz)	Measured Frequency (MHz)	Relative Error
1	17.09	17.39	$1.8 \cdot 10^{-2}$
2	45.09	45.06	7.0×10^{-4}

As an example for a cavity with a dielectric insert, we use the rectangular cavity loaded by a Teflon tube[9] as shown in Fig. 8. Measured and calculated results agree very well, as can be seen in Table III.

TABLE III

Measured and Calculated Lowest Resonant Frequencies of a Dielectric-Loaded (Teflon Tube) Rectangular Cavity (see Fig. 8)

	Frequency (MHz)		
	Measured	Calculated, $N_3 = 690$	Calculated, $N_3 = 3185$
With dielectric tube	1258	1255	1256
Without dielectric tube	1319	1310	1319

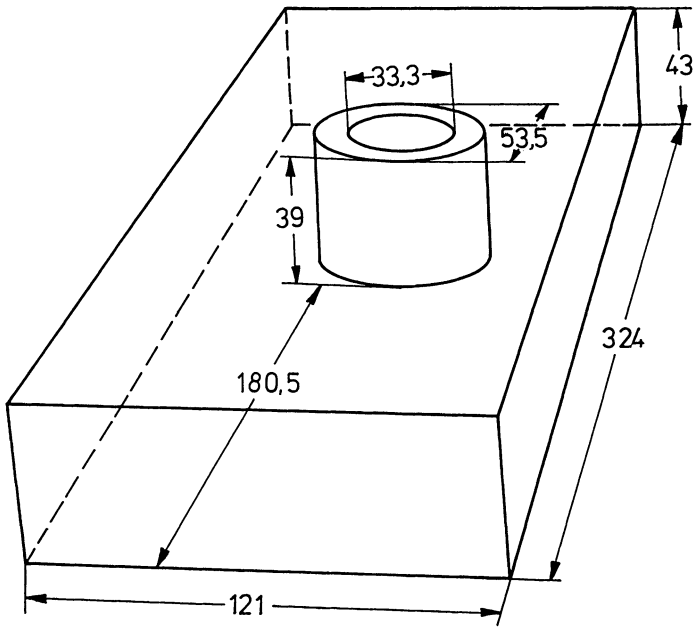

FIGURE 8 Rectangular cavity loaded with a dielectric tube.

THE COMPUTER PROGRAM

A preliminary computer program has been prepared that can handle up to 40,000 nodes on an IBM 3081 using about 30 minutes cpu time for the ten lowest modes. The cpu time scales as $N^{1.5}$ with N the total number of mesh points (see Fig. 9).

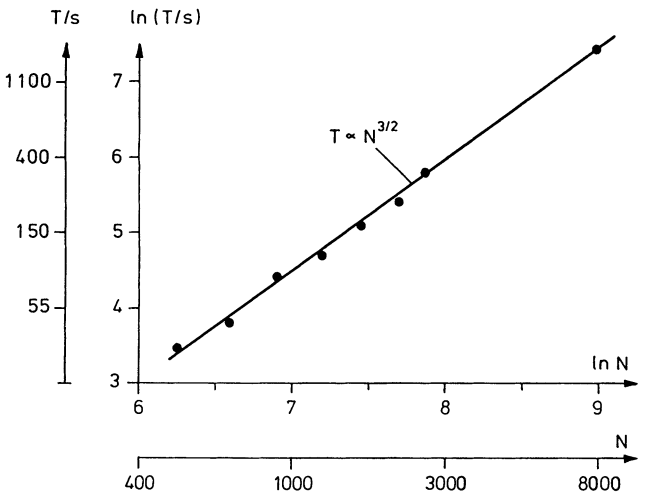

FIGURE 9 cpu time T on an IBM 3081 D in seconds as function for number of nodes.

This code is part of a family of $3D$-codes (called MAFiA) and shares input and output facilities with other programs.

A joint effort between Los Alamos National Laboratory, Kernforschungsanlage Jülich and DESY has been started in order to prepare a much more user-friendly and a much-faster code within the near future.

ACKNOWLEDGEMENTS

The author wishes to thank D. Barber and R. Klatt for careful reading of the manuscript and for many useful hints. Also thanks are due to B. Dwersteg for doing the measurements of the dielectric cavity and to R. K. Cooper who made available to me the measurements performed at Los Alamos National Laboratory.

LITERATURE

1. T. Weiland, "Design of r.f. cavities", Lecture Notes in Physics **215** (1983), 21–32.
2. H. Albani and M. Bernardi, "A numerical method on the discretization of Maxwell's equations in integral form", *IEEE*, MTT22 (1974), 446–449.
3. W. Wilhelm, "CAVIT and CAV3D—Computer Programs for rf-cavities with constant cross section or any three dimensional form", *Particle Accelerator* **12** (1982), p. 139.
4. M. Hara, T. Wada, A. Toyanna, F. Kikuchi, "Calculation of RF Electromagnetic Field by Finite Element Method", Scientific Papers of the Institute of Physical and Chemical Research 75 (1982), 143–175 and D. T. Tran, A. Cailleaux and G. Berthevas, Proceedings of the 1984 Linear Accelerator Conference GSI-84-11, Darmstadt, 1984, pp. 414–416.
5. T. Weiland, "A Discretization Method for the Solution of Maxwell's Equations for Six-Component Fields", *AEÜ* **31** (1977), p. 116–120.
6. T. Weiland, "On the Numerical Solution of Maxwell's Equations and Applications in the Field of Accelerator Physics", *Particle Accelerator* **15** (1984), pp. 245–292.
7. T. Weiland, "On the Computation of Resonant Modes in Cylindrically Symmetric Cavities", *NIM* **216** (1983), pp. 329–348.
8. These measurements have been performed by group AT1, Los Alamos National Laboratory, (results were scaled from inches to meters)
9. These measurements were performed by B. Dwersteg, DESY.

APPENDIX A

In order to prove that a time harmonic rotational solution in the grid is implicitly source free we rewrite Eq. (21) (setting $\mathbf{D}_{\tilde{s}} = \mathbf{D}_{\tilde{\mu}}^{-1} = \mathbf{D}_{\tilde{A}} = \mathbf{D}_{\tilde{\epsilon}} =$ unit matrix for simplicity):

$$-\mathbf{A}_w \mathbf{b}_v + \mathbf{A}_v \mathbf{b}_w = \frac{\omega}{c} \cdot \mathbf{e}_u \tag{A1}$$

$$\mathbf{A}_w \mathbf{b}_u - \mathbf{A}_u \mathbf{b}_w = \frac{\omega}{c} \cdot \mathbf{e}_v \tag{A2}$$

$$-\mathbf{A}_v \mathbf{b}_u + \mathbf{A}_u \mathbf{b}_v = \frac{\omega}{c} \cdot \mathbf{e}_w \tag{A3}$$

with

$$\mathbf{e} = (\mathbf{e}_u, \mathbf{e}_v, \mathbf{e}_w)^* \tag{A4}$$

$$\mathbf{b} = (\mathbf{b}_u, \mathbf{b}_v, \mathbf{b}_w)^* \tag{A5}$$

We multiply these three equations by $\mathbf{A}_u$, $\mathbf{A}_v$ and $\mathbf{A}_w$ and sum up to the result:

$$\begin{aligned}\frac{\omega}{c} \cdot (\mathbf{A}_u\mathbf{e}_u + \mathbf{A}_v\mathbf{e}_v + \mathbf{A}_w\mathbf{e}_w) &= \left(\frac{\omega}{c}\right) \cdot (\mathbf{S} \cdot \mathbf{e}) \\ &= (\mathbf{A}_v\mathbf{A}_w - \mathbf{A}_w\mathbf{A}_v)\mathbf{b}_u \\ &+ (\mathbf{A}_w\mathbf{A}_u - \mathbf{A}_u\mathbf{A}_w)\mathbf{b}_v \\ &+ (\mathbf{A}_u\mathbf{A}_v - \mathbf{A}_v\mathbf{A}_u)\ \mathbf{b}_w \equiv \mathbf{0},\end{aligned} \tag{A6}$$

since one easily verifies that

$$\mathbf{A}_u\mathbf{A}_v = \mathbf{A}_v\mathbf{A}_u;\ \mathbf{A}_u\mathbf{A}_w = \mathbf{A}_w\mathbf{A}_u;\ \mathbf{A}_v\mathbf{A}_w = \mathbf{A}_w\mathbf{A}_v. \tag{A7}$$

Thus it follows that for any solution $\mathbf{e}$ we have

$$\text{either A)}\ \omega = 0, \qquad \mathbf{S} \cdot \mathbf{e} \neq 0 \quad \text{or} \quad \mathbf{S} \cdot \mathbf{e} = 0$$

$$\text{or B)}\ \omega \neq 0, \qquad \mathbf{S} \cdot \mathbf{e} \equiv 0$$

i.e. any time harmonic grid solution of the curl equations is implicitly source free, which follows from the special discretization ansatz used. A similar proof is found to show that every rotational time harmonic magnetic field is source free as well.

APPENDIX B

We rewrite Eqs. (18) and (19) using (22) as

$$\mathbf{C}^*\mathbf{D}_s\mathbf{e} = \frac{\omega}{c}\mathbf{D}_A\mathbf{b}, \tag{B1}$$

$$\mathbf{C}\mathbf{D}_s\mathbf{D}_\mu^{-1}\mathbf{b} = \frac{\omega}{c}\mathbf{D}_\varepsilon\mathbf{D}_{\tilde{A}}\mathbf{e}. \tag{B2}$$

With the formal equations:

$$\mathbf{b} = \mathbf{D}_\mu\mathbf{h}, \qquad k = \omega/c \tag{B3}$$

we find

$$\mathbf{C}^*\mathbf{D}_s\mathbf{e} = k\mathbf{D}_A\mathbf{D}_\mu\mathbf{h}, \tag{B4}$$

$$\mathbf{C}\mathbf{D}_{\tilde{s}}\mathbf{h} = k\mathbf{D}_{\tilde{A}}\mathbf{D}_\varepsilon\mathbf{e}. \tag{B5}$$

We perform the same transformation as Eq. (25) but also for the magnetic field:

$$\mathbf{e}' = (\mathbf{D}_\varepsilon\mathbf{D}_{\tilde{A}}\mathbf{D}_s)^{1/2}\mathbf{e}, \tag{B6}$$

$$\mathbf{h}' = (\mathbf{D}_\mu\mathbf{D}_A\mathbf{D}_{\tilde{s}})^{1/2}\mathbf{h}. \tag{B7}$$

and obtain

$$\mathbf{C}^*\mathbf{D}_s^{1/2}\mathbf{D}_\varepsilon^{-1/2}\mathbf{D}_A^{-1/2}\mathbf{e}' = \mathbf{D}_A^{1/2}\mathbf{D}_\mu^{1/2}\mathbf{D}_{\tilde{s}}^{-1/2}\mathbf{h}', \tag{B8}$$

$$\mathbf{C}\ \mathbf{D}_{\tilde{s}}^{1/2}\mathbf{D}_\mu^{-1/2}\mathbf{D}_A^{-1/2}\mathbf{h}' = k\mathbf{D}_{\tilde{A}}^{1/2}\mathbf{D}_\varepsilon^{1/2}\mathbf{D}_s^{-1/2}\mathbf{e}'. \tag{B9}$$

Or with the abbreviation of Eq. (27) and (28)

$$\mathbf{C}^*\tilde{\mathbf{D}}\mathbf{e} = k\mathbf{D}^{-1}\mathbf{h}', \tag{B10}$$

$$\mathbf{C}\ \mathbf{D}\mathbf{h} = k\tilde{\mathbf{D}}^{-1}\mathbf{e}'. \tag{B11}$$

We multiply Eq. (A10) by $\mathbf{D}$ from the left and Eq. (A11) by $\tilde{\mathbf{D}}$, we put $\mathbf{h}'$ and $\mathbf{e}'$ into one vector and find:

$$\begin{pmatrix} \mathbf{0} & \mathbf{D}\mathbf{C}^*\tilde{\mathbf{D}} \\ \tilde{\mathbf{D}}\mathbf{C}\mathbf{D} & \mathbf{0} \end{pmatrix} \quad \begin{pmatrix} \mathbf{h}' \\ \mathbf{e}' \end{pmatrix} = k \begin{pmatrix} \mathbf{h}' \\ \mathbf{e}' \end{pmatrix} \tag{B12}$$

The matrix of the eigenvalue problem in k is real and symmetric. Thus k is real and k^2 positive or zero. Thus Eq. (35) has a semi positively defined matrix.